

MAGNETIC BIREFRINGENCE STUDIES OF DILUTE PURPLE MEMBRANE SUSPENSIONS

BARBARA A. LEWIS,* CHARLES ROSENBLATT,* ROBERT G. GRIFFIN,* JAMES COURTEMANCHE,[‡]
AND JUDITH HERZFELD[‡]

*Francis Bitter National Magnet Laboratory, Massachusetts Institute of Technology, Cambridge,
Massachusetts 02139; and [‡]Department of Physiology and Biophysics, Harvard Medical School,
Boston, Massachusetts 02115

ABSTRACT We have observed the magnetically induced orientation of purple membrane suspensions by measuring the birefringence as a function of concentration and temperature at fields up to 10.5 Tesla (T). At these fields, the orientation approaches saturation even in dilute solutions; therefore, the birefringence data, together with an estimate of the membrane size distribution obtained from electron microscopy, permits one to determine the diamagnetic susceptibility anisotropy. We find $\Delta\chi_{\text{mole}} = 1.2 \pm 0.3 \times 10^{-3} \text{ erg G}^{-2}\text{mol}^{-1}$ of bacteriorhodopsin. If $\Delta\chi$ were due only to the oriented peptide bonds of the transmembrane alpha helices, this experimental value would indicate that ΔK , the anisotropy per mole of peptide bonds, is considerably larger than previously suggested. On the other hand, the large value for $\Delta\chi_{\text{mole}}$ of bacteriorhodopsin can also be explained by a net orientation of the aromatic amino acid side chains of bacteriorhodopsin with their planes perpendicular to the membrane surface. In addition, the present data analysis demonstrates the critical dependence of the calculated $\Delta\chi$ value on the values for the membrane size distribution.

INTRODUCTION

Purple membranes are patches of the cell membrane of the *Halobacterium halobium* (*H. halobium*) that contain a single protein, bacteriorhodopsin (BR), interspersed with lipid molecules in a molar ratio of ~1:12 (Oesterhelt and Stoekenius, 1971). The normal growth medium for *H. halobium* contains 4.3 M salt; resuspension of the cells in distilled water causes them to lyse and most of the cell membrane to disintegrate. Only the purple membrane remains intact, and thus these specialized fragments are readily purified.

BR is a light-driven proton pump and its function, structure, and photocycle have been extensively investigated (for reviews see Henderson, 1977; Stoekenius, 1980; Wallace, 1982; Stoekenius and Bogomolni, 1982). Because the protein molecules form a two-dimensional hexagonal lattice in the plane of the membrane, electron diffraction analysis has been possible. The pioneering three-dimensional reconstruction work of Henderson and Unwin (1975) shows the BR monomer to consist of seven rods traversing the membrane at angles to the membrane normal from 0 to ~20°. The 248 amino acid sequence of the protein has been determined (Khorana et al., 1979; Ovchinnikov et al., 1979), and there is substantial evidence that most of the secondary structure is alpha helix (Blau-

rock, 1975; Henderson, 1975, and see above reviews). However, it has also been proposed that a significant fraction is beta sheet (Jap et al., 1983).

The general phenomenon of orientation of anisotropic macromolecular assemblies in magnetic fields has been known for some time, as has the fact that purple membranes in aqueous suspension orient with the membrane planes perpendicular to the magnetic field direction (Neugebauer et al., 1977). Such orientation results from anisotropy of the diamagnetic susceptibility, which arises from an anisotropic arrangement of chemical bonds. Of the known types of protein secondary structure, alpha helices have the highest diamagnetic anisotropy (Worcester, 1978), and since purple membranes contain a very closely packed transmembrane protein that is largely alpha helical in nature, this behavior is not surprising.

To characterize the magnetic orientation behavior of purple membrane suspensions in more detail, we have measured the birefringence (which is a function of degree of orientation) vs. concentration, temperature, and magnetic field strength from 0 to 10.5 Tesla (T) (1T = 10 kilogauss). At these relatively high field strengths, the orientation approaches saturation, eliminating errors that may arise from the necessity to determine the saturated birefringence by other methods. In addition, in the dilute limit, these measurements yield a value of the total magnetic susceptibility anisotropy per particle, which is independent of sample concentration. Thus, errors in the measurement of sample concentration have no effect.

These experiments have two goals. First, the birefrin-

Correspondence should be addressed to Dr. Charles Rosenblatt.
Dr. Lewis' present address is the Biology Division, Oak Ridge National
Laboratory, Oak Ridge, TN 37830.

gence data for dilute suspensions, where the fragments behave as noninteracting individual particles, permit us to determine the diamagnetic anisotropy, $\Delta\chi$, per unit volume of membrane. This value can subsequently be interpreted in terms of the orientations of molecular species within the membranes. Second, at higher concentrations, where the fragments begin to interact, a detailed study of the concentration dependence of the magnetic orientation can elucidate the nature of these intermembrane interactions. Here only the dilute concentration regime has been analyzed in detail; studies of more concentrated samples will be reported in a future publication.

MATERIALS AND METHODS

Sample Preparation

H. halobium strain R1 was grown in a defined growth medium (Argade et al., 1981). The culture was harvested at the end of the logarithmic growth phase and purple membrane was isolated by the method of Oesterhelt and Stoekenius (1974). After sucrose density gradient centrifugation, the purple membranes were washed several times in deionized distilled water. The membranes were pelleted at 43,000 *g* and resuspended in a minimal amount of water; this concentrated suspension was diluted to produce samples ranging from 1.1 to 11.1 mg/ml. Sample concentrations were determined by measurement of optical absorbance at 560 nm using an extinction coefficient of 1.8 $\text{cm}^{-1}/(\text{mg purple membrane/ml})$. The samples were kept at 2–4°C until use, and all experiments were carried out within several days after removal from the sucrose gradient to minimize sample aggregation and bacterial contamination.

The size and shapes of the purple membrane fragments were determined by transmission electron microscopy. The samples were deposited onto Parlodion-coated grids, rinsed, stained with 0.5% uranyl acetate, allowed to dry, and examined in an electron microscope (EM 201, Philips Electronic Instruments, Inc., Mahwah, NJ). Prints were made of several randomly chosen areas of two different grids, and all clearly distinguished fragments (92 total) were measured.

Magnetic Birefringence Measurements

The membrane suspensions were placed in a glass cuvette of path length $l = 0.1$ cm, which was housed in a cylindrical brass oven equipped with a small transverse optical port. The oven was surrounded in turn by a Teflon insulator and copper cooling coils through which refrigerated water was pumped. Temperature was controlled by a pair of thermistors (UUA33J4, Fenwal Electronics, Framingham, MA) and a temperature controller (model 72, Yellow Springs Instrument Co., Yellow Springs, OH). For these experiments overall temperature control was about ± 50 mK, including magnetorestrictive effects in the feedback thermistor. The oven assembly was placed in the axial bore of a 10.7 T Bitter magnet, which possessed a 2.5 cm diam. transverse optical bore. The sample was illuminated with an He-Ne laser (model 124B, Spectra-Physics, Inc., Mountain View, CA) (wavelength = 6,328 Å), attenuated to 0.8 mW. When the samples were removed from the light beam, the area through which the beam had passed was observed to be slightly darker and bluer in color than the rest of the sample, indicative of light adaptation. Under these illumination conditions and at room temperature, each BR molecule spends at most 10% of its time photocycling.

To measure the degree of field-induced orientational order, an automatically compensating optical birefringence scheme was utilized (Rosenblatt and Ho, 1982; Rosenblatt, 1984). The apparatus, which was based upon a compensating Pockels cell modulated by a small voltage at 2.8 kHz, had a phase sensitivity of $\sim 3 \times 10^{-4}$, corresponding to a birefringence sensitivity of $\Delta n = 3 \times 10^{-8}$ for $l = 0.1$ cm. The compensating voltage applied to the Pockels cell, which is proportional to

the birefringence, was plotted vs. H^2 on an *x-y* recorder. The electronics response time was ultimately limited by the 1 s smoothing filter in the magnet electronics, but this was still fast relative to the total sweep duration. Because the field was swept from 0 to 10.5 T over periods of time ranging from 10 min for the sample of lowest concentration to 50 min at the highest concentration, drifts of the birefringence baseline could be observed. These drifts were typically of the order $\Delta n = 5 \times 10^{-7}$, or $\sim 1\%$ of the saturated birefringence for the 1.1 mg/ml sample.

A potential source of experimental difficulty was the presence of circular dichroism, which has the effect of introducing a small amount of ellipticity in addition to that due to the linear birefringence. From the work of Heyn et al. (1975), the effective phase shift in zero field was expected to be $< 10^{-4}$, which is very small relative to our experimental results. We thus exclude circular dichroism from further consideration.

RESULTS AND ANALYSIS

Δn vs. H^2 was recorded for samples at five concentrations (1.1, 2.2, 4.3, 8.2, and 11.1 mg/ml), each at several temperatures between 8.5 and 37.0°C. A typical experimental trace for low concentration is shown in Fig. 1. The slope $d(\Delta n)/d(H^2)$ in the trace does not decrease monotonically with H^2 but rather rises for small H^2 , reaches a maximum in the neighborhood of 8–10 T^2 , and then begins to fall off. This very slight nonlinear behavior is in excellent agreement with theory (see Eq. 3 below) and, in fact, the presence of an inflection point has been previously used to analyze fluorescence data from *Chlorella* (Knox and Davidovich, 1978).

For the highest concentration sample (11.1 mg/ml), Δn rose very sharply just above $H^2 = 0$, achieving about one half of its saturated value at H^2 between 3 and 5 T^2 . For this sample the orientational relaxation time, as determined by the decay of Δn when the field was brought rapidly back to zero, was quite long (several minutes). Thus, it is possible that sweeps even slower than 50 min would be required for an accurate study of the high concentration samples.

With decreasing concentration, both the relaxation times and the initial slopes decreased, so that by 2 mg/ml the relaxation time was faster than the electronics response time and no hysteresis was observed when the field was swept down from 10.5 to 0 T. More importantly, however,

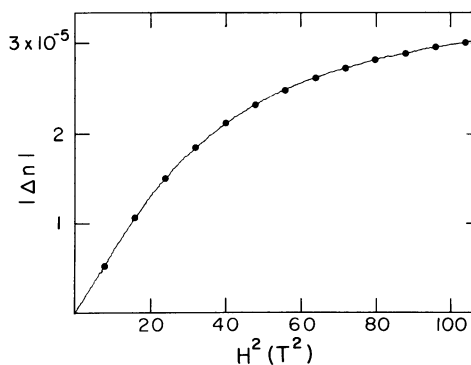


FIGURE 1 Birefringence vs. H^2 (Tesla²). Curve: experimental trace for 1.1 mg/ml sample at 29.7°C. Circles: two-parameter fit to the data (Eq. 3) using the measured distribution of fragment areas.

the curves rapidly approached a limiting shape identical to that obtained at 1.1 mg/ml (see Fig. 1). In this paper, we shall confine our discussion to these results, which yield information about the magnetic properties of the individual membranes as well as their optical properties in suspension. Quantitative experiments on more concentrated samples, which yield information on membrane-membrane interactions, are still underway.

In the infinitely dilute case, a membrane fragment interacts only with the magnetic field. For purposes of analysis, the membrane fragments are assumed to be flat and rigid, with the symmetry axis perpendicular to the membrane surface. Thus, for a fragment of area A_i , thickness t , and magnetic susceptibility anisotropy per unit volume $\Delta\chi$, the orientationally-dependent part of the free energy is $F_o = -(1/2)\Delta\chi A_i t H^2 \cos^2 \theta$ (DeGennes, 1975), where θ is the angle between the symmetry axis and the field. Because it has been found experimentally by neutron scattering (Neugebauer et al., 1977) and nuclear magnetic resonance (Lewis, B. A., D. M. Rice, J. Herzfeld, and R. G. Griffin, unpublished results) that purple membranes orient with the symmetry axis along H , we conclude that $\Delta\chi > 0$.

The strong optical birefringence Δn of oriented samples arises primarily from two sources: the inherent birefringence of the membrane deriving from the anisotropy of the polarizability of its constituent molecules, and the form birefringence, originating from electromagnetic boundary conditions at the surfaces of the membrane fragments (Born and Wolf, 1980). For membranes of uniform thickness, the saturation birefringence scales with total area. For the 1.1 mg/ml sample, the measured saturated birefringence ($H^2 \rightarrow \infty$) was about -3.5×10^{-5} , in close agreement with the results of a calculation for the form birefringence (Born and Wolf, 1980, p. 705) for a 1.1 mg/ml suspension of perfectly aligned thin plates of refractive index 1.5 (Brith-Lindner and Rosenheck, 1977) in distilled water ($n = 1.33$). Thus, the form birefringence dominates for purple membranes.

To quantitatively interpret the measurements, we note that the net sample birefringence is given by

$$\Delta n = \sum_{i=1}^N \Delta n_o A_i \langle P_2(\cos \theta) \rangle_i \quad (1)$$

where N is the number of fragments illuminated by the laser, Δn_o is the contribution to the birefringence per unit fragment area of a fully aligned membrane fragment, and $P_2(\cos \theta)$ is the second Legendre polynomial (DeGennes, 1975), i.e., $P_2(\cos \theta) = 3/2 \cos^2 \theta - 1/2$. $\langle P_2(\cos \theta) \rangle_i$ represents the degree of field-induced order of fragment i and is given by the Boltzmann distribution. For an individual fragment of area A_i ,

$$\langle P_2(x) \rangle_i = \frac{\int_0^1 \left(\frac{3}{2} x^2 - \frac{1}{2} \right) \exp(b_o A_i H^2 x^2) dx}{\int_0^1 \exp(b_o A_i H^2 x^2) dx}, \quad (2)$$

where $b_o = \Delta\chi t / 2k_B T$, k_B is Boltzmann's constant and T is temperature. Note that b_o represents the susceptibility anisotropy per unit fragment area divided by $k_B T$. It is assumed that the fragment thickness t is uniform. Combining Eqs. 1 and 2, and writing the integrals in terms of Dawson's function (Abramowitz and Stegun, 1972), we obtain

$$\Delta n(H^2) = \sum_{i=1}^N \Delta n_o A_i \left\{ \frac{3[(\sqrt{b_o A_i H^2}) - D(\sqrt{b_o A_i H^2})]}{4b_o A_i H^2 D(\sqrt{b_o A_i H^2})} - \frac{1}{2} \right\}, \quad (3)$$

where

$$D(x) = e^{-x^2} \int_0^x e^{t^2} dt. \quad (4)$$

From Eq. 3, it is clear that the fragment area has two effects: larger fragments, with a larger net susceptibility anisotropy ($\propto b_o A_i$) will have an orientational distribution more sharply peaked $\sim \theta = 0$; in addition, fragments of larger area contribute proportionately more ($\propto \Delta n_o A_i$) to the total birefringence. Thus, to obtain the two-fitted parameters Δn_o and b_o , it is necessary to have a knowledge of the distribution of fragment areas A_i . To this end, the 1.1 mg/ml sample was examined by electron microscopy, which showed that most of the membranes were roughly oval in shape and that the distribution of fragment sizes was quite wide, as shown in Fig. 2. Membranes with linear dimensions from 0.25 to 2.2 μm were observed, with a mean of 0.75 μm . The area distribution was skewed to lower areas, peaking at $\sim 0.25 \mu\text{m}^2$ and trailing off slowly at the high end. The arithmetic mean of the area distribution for the 92 fragments measured was 0.46 μm^2 with a standard deviation of 0.28 μm^2 .

A two parameter ($\Delta n_o \sum_i A_i$, b_o) fit of Eq. 3 was performed using both the birefringence data and the electron microscopic area data, assuming that the size distribution determined from the measured fragments was

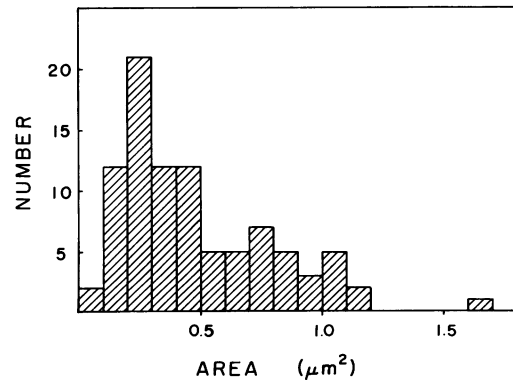


FIGURE 2 Area distribution of purple membrane fragments in the experimental sample, determined by transmission electron microscopy of uranyl acetate-stained samples for 92 fragments.

representative of the entire sample. The fit was performed for data at all concentrations to determine the concentration regime for which the noninteracting model is valid. At any given temperature it was found that the fitted value for the saturated birefringence, $\Delta n_o \Sigma_i A_i$, scaled approximately as the concentration, as expected. On the other hand, the effective b_o was found to decrease rapidly with decreasing concentration, approaching a constant at low concentrations. Specifically, $b_o(8.2 \text{ mg/ml})/b_o(4.3 \text{ mg/ml})/b_o(2.2 \text{ mg/ml})/b_o(1.1 \text{ mg/ml})$ was $\sim 5.8:1.6:1.09:1.0$ at room temperature. The results suggest that the effective b_o values at higher concentrations include an interaction component to F_o , while at the lowest concentration these interactions are vanishingly small. The remainder of this paper will deal exclusively with the noninteracting regime, i.e., 1.1 mg/ml.

The filled circles in Fig. 1 indicate points along a least-squares fit to the data. Table I shows the fitted values for both b_o and the saturated birefringence ($=\Delta n_o \Sigma_i A_i$) for the 1.1 mg/ml sample as a function of temperature. Two features are immediately apparent. First, although b_o is expected to scale as $1/T$, it in fact falls off more rapidly, decreasing by 20% when $1/T$ decreased by only 10%. In Fig. 3, the fitted b_o values are represented by circles and the dotted line is that expected for a simple $1/T$ dependence, normalized to the experimental b_o value at 22.6°C. Possible causes of this deviation are considered in the Discussion section. A second notable feature of the data in Table I is the constancy of the saturated birefringence with temperature. This result is expected for fragments for which the shape and rigidity remain constant with temperature. In addition, it should be noted that the fit is quite

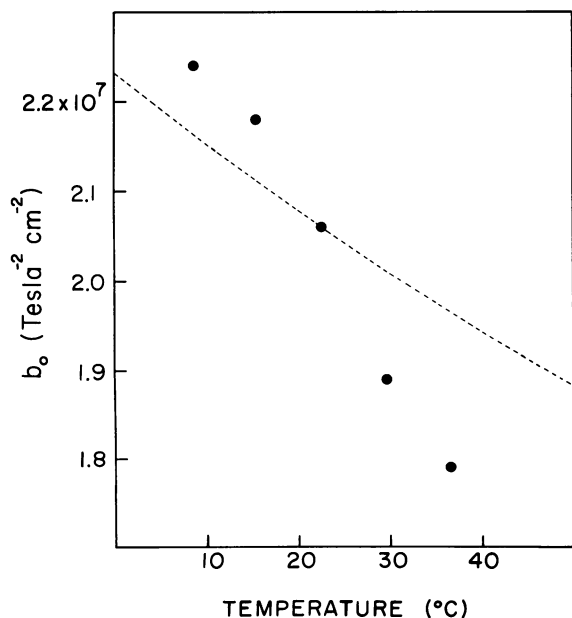


FIGURE 3 b_o vs. temperature. Circles: values from the two-parameter fit to the experimental data for the 1.1 mg/ml sample. Dotted line: calculated $1/T$ dependence, scaled to the fitted value at 22.6°C.

TABLE I
PARAMETERS FROM FIT TO DATA FOR 1.1 mg/ml
SAMPLE

Temperature	b_o	Saturated birefringence
°C	$T^{-2} \text{cm}^{-2}$	
8.60 ± 0.05	$2.25 \pm 0.02 \times 10^7$	$-3.48 \pm 0.02 \times 10^{-5}$
15.26	2.18	-3.53
22.56	2.06	-3.50
29.71	1.89	-3.53
36.56	1.79	-3.48

sensitive; changing b_o or Δn_o by 1% from the fitted values more than doubles the rms deviation of the fit, making it larger than the experimental error.

Given values of b_o of $\sim 2.1 \times 10^7 \text{ T}^{-2} \text{ cm}^{-2}$, $\Delta \chi$ can immediately be calculated. Using $k_B T = 4.1 \times 10^{-14} \text{ erg}$ and membrane thickness $4.9 \times 10^{-7} \text{ cm}$ (Blaurock, 1975), we find $\Delta \chi$ (per unit volume) = $3.5 \text{ erg cm}^{-3} \text{ Tesla}^{-2} = 3.5 \times 10^{-8} \text{ erg cm}^{-3} \text{ G}^{-2}$ (gauss) (cgs units). Because there are three BR molecules per 63 \AA unit cell of the hexagonal lattice of purple membrane (Blaurock and Stoeckenius, 1971), there is one molecule per $1,146 \text{ \AA}^2$; for a 49 \AA thick membrane (Blaurock and Stoeckenius, 1971), each $5.6 \times 10^{-20} \text{ cm}^3$ contains one molecule. Thus, $\Delta \chi_{\text{mole}}$ ($\Delta \chi$ per mole of BR) = $1.2 \times 10^{-3} \text{ erg mol}^{-1} \text{ G}^{-2}$.

DISCUSSION

From the above analysis of high-field magnetic birefringence data on a 1.1 mg/ml suspension of purple membrane fragments, a diamagnetic anisotropy value of $\Delta \chi_{\text{mole}} = 1.2 \times 10^{-3} \text{ erg G}^{-2}$ per mole of bacteriorhodopsin has been calculated. We now interpret this experimental result in light of what is known about the structure of purple membrane. Significant contributions to the diamagnetic anisotropy of the membrane are to be expected from three groups: the peptide bonds of BR, the lipid molecules, and the aromatic side chains of BR. Note that because of the threefold symmetry of the BR lattice in native purple membrane, the symmetry axis of the diamagnetic susceptibility tensor due to the protein must be strictly normal to the membrane surface; any in-plane components will cancel out.

Worcester (1978) suggested that the dominant contribution to $\Delta \chi$ for proteins such as BR is that of the peptide bonds and showed that for an alpha helix perpendicular to the membrane plane, $\Delta \chi_{\text{mole}} = N \Delta K / 2$, where ΔK is the diamagnetic anisotropy per mole of peptide bonds and N is the number of residues. For beta sheet also oriented perpendicular to the membrane $\Delta \chi_{\text{mole}} = N \Delta K / 8$; thus substitution of beta sheet (in any orientation) for alpha helix will reduce the diamagnetic anisotropy of the protein. If the transmembrane alpha helices of BR indeed dominate the diamagnetic anisotropy of purple membrane, then we can calculate the peptide bond ΔK from the experimental $\Delta \chi$ value. Using a reasonable upper limit of 210 residues in

alpha helices normal to the membrane surface (30 in each of 7 helices), we calculate $\Delta K_{\text{peptide}} \approx 1.1 \times 10^{-5} \text{ erg G}^{-2} \text{ mol}^{-1}$. For 175 helical residues (25×7), we obtain 1.4×10^{-5} , and for the (unlikely) case in which all 248 residues are in the helices, we obtain $9.7 \times 10^{-6} \text{ erg G}^{-2} \text{ mol}^{-1}$.

All these values are considerably larger than those previously suggested either on theoretical grounds ($5.36 \times 10^{-6} \text{ erg G}^{-2} \text{ mol}^{-1}$ by Pauling [1979]) or by experimental data ($8.8 \times 10^{-6} \text{ erg G}^{-2} \text{ mol}^{-1}$ by Worcester [1978]; $3.7 \times 10^{-6} \text{ erg G}^{-2} \text{ mol}^{-1}$ by Murthy et al. [1976]). Also, Torbet and Maret (1981) state that their experimental results on phages are more consistent with the lower two of the above three estimates. These discrepancies suggest either that all previous values for the peptide bond ΔK are too small, or that other groups in the membrane are also oriented so as to increase the net $\Delta\chi$. The next paragraphs discuss the latter possibility, whereas to verify the first possibility, further experiments on well-defined polypeptides with a wide range of side chains would be useful.

The contribution to $\Delta\chi_{\text{mole}}$ from the lipid molecules cannot be calculated exactly in the absence of experimental data for the diamagnetic anisotropy of ether-linked diphytyl lipids. However, for rough estimates we will use the values of $\Delta\chi_{\text{mole}} = -2.4 \times 10^{-5}$ for dimyristoyl lecithin bilayers (Scholz et al., 1984) and $\Delta\chi_{\text{mole}} = -7 \times 10^{-6}$ for egg lecithin bilayers (Boroske and Helfrich, 1978). Higher values have been obtained for crystalline lipid systems (Sakurai et al., 1980), but the values for disordered bilayers are more appropriate here, given that in hydrated purple membranes the phospholipids undergo fairly rapid long-axis rotation (Ekiel et al., 1981) and that the hydrocarbon chains are not highly ordered. Because of the small lipid content of purple membrane, the lipid contribution calculated using these values is about a factor of three to fifteen smaller than the experimental $\Delta\chi$ and thus cannot be a major factor. Note that the lipid contribution opposes that of the protein helices, so that oriented groups in the protein must make an even larger contribution than discussed above. Finally, the contribution of one retinal moiety per 10 lipid molecules, 30 aromatic groups, and 247 peptide bonds is expected to be negligible.

On the other hand, the contribution to $\Delta\chi_{\text{mole}}$ of the protein aromatic groups can be quite significant: from the molar diamagnetic anisotropy of benzene, $\Delta K = 54 \times 10^{-6} \text{ erg G}^{-2}$ (Worcester, 1978), we find that if all 24 tyrosine and phenylalanine rings were oriented with their planes perpendicular to the bilayer, an additional $\Delta\chi_{\text{mole}}$ of 1.3×10^{-3} would be obtained. This is more than enough to bring $\Delta\chi$ up to the experimental value. In addition, the eight tryptophans at $\Delta K = 86 \times 10^{-6}$ (Torbet and Maret, 1981) can contribute $\Delta\chi_{\text{mole}}$ up to 0.7×10^{-3} . Thus, our results are consistent with a net orientation of about one third of the aromatic side chains with their planes perpendicular to the membrane surface, if we use Pauling's value for the peptide bond ΔK and an estimated 25 residues per helix. Evidence for orientation of aromatic rings with their planes

parallel to the axis of alpha helices has been found for at least two other proteins, the coat proteins of phages (Torbet and Maret, 1981) and fd (Cross and Opella, 1983). Thus, such orientations in the case of BR would not seem unreasonable.

One test of the orientation of the aromatic side chains of BR with respect to the membrane surface is the measurement of ultraviolet linear dichroism of oriented purple membranes. Such a measurement by Breton (dissertation, cited by Worcester [1978]) indicated a net orientation of the aromatic side chains in the opposite direction (parallel to the membrane plane) from that suggested by the present magnetic orientation results. If the majority of the aromatic rings are in fact oriented parallel to the membrane plane, then the only remaining explanation for the large experimental value for $\Delta\chi_{\text{mole}}$ of BR is that the correct value for $\Delta\chi$ per mole of peptide bonds is indeed considerably larger than all previous suggestions. However, an alternative explanation is that the UV dichroism is dominated by the eight tryptophan residues, while the 24 tyrosine and phenylalanine rings, which have much smaller extinction coefficients, may be oriented differently from the tryptophan side chains and outweigh them in the measured diamagnetic anisotropy. Several groups have reported dichroic changes in the appropriate wavelength region during the photocycle of BR (Becher et al., 1978; Hess and Kuschnitz, 1979; Bogomolni et al., 1978; Fukumoto and El-Sayed, 1983; Draheim et al., 1984). These changes should be reflected in changes in b_o ($\Delta\chi$) during the photocycle if aromatic group orientations dominate the diamagnetic anisotropy, as suggested by the present results. Thus, it will be informative to repeat the present experiments under conditions in which the photointermediates are more heavily represented.

As part of this analysis, it is important to assess the accuracy of the experimental value for $\Delta\chi$. Assuming that experimental error such as baseline drifts in the electronics are negligible (see Materials and Methods), the major sources of error in obtaining $\Delta\chi$ (per volume) are the determinations of the size distribution of the purple membrane fragments and of the membrane thickness. In calculating $\Delta\chi_{\text{mole}}$ from $\Delta\chi$, the membrane thickness again enters the calculation, so that errors in this parameter will cancel out. Also included here are the lattice dimensions, which are known to high precision. Since sample concentration does not enter the calculation at all, the predominant source of error in the overall calculation therefore comes from the area distribution, which in fact makes a critical contribution, as shown below.

Two preliminary analyses of the magnetic birefringence data were carried out. In the first, a two-parameter (susceptibility anisotropy and saturated birefringence) fit was performed assuming that the purple membrane fragments were uniform in size, and in the second, the area distribution was represented by a Gaussian distribution with the width of the Gaussian being a third parameter of

the fit to the data. These two treatments gave $\Delta\chi_{\text{mole}}$ values of $\sim 1.7 \times 10^{-3}$ and differed from each other by only $\sim 15\%$. However, because the measured area distribution was highly asymmetric (see Fig. 2), it was deemed more appropriate to include the actual area data rather than a poor functional representation. As presented above, this treatment yields a $\Delta\chi_{\text{mole}}$ value of 1.2×10^{-3} , considerably lower than that obtained assuming either uniform fragment size or a simple Gaussian distribution. These results clearly show that errors in the assumed shape of the area distribution will be reflected in the $\Delta\chi$ values obtained from fits to the birefringence data.

Because the data analysis presented above uses the measured area data, one can readily assess the quantitative effects of errors in the area measurements. When the largest fragment in the population (Fig. 2) was excluded in performing the fit to the magnetic birefringence data, the value for b_o increased by $\sim 5\%$; when six fragments were added to fill the gap in the distribution between 1.1 and 1.6 μm^2 , the value decreased by 15%. Thus, as expected, the calculated values are quite sensitive to errors in the area distribution, especially at the high end of the distribution, and one can estimate that the standard deviation of the final $\Delta\chi_{\text{mole}}$ value is 20–25% due to statistical errors in the area measurements. However, since the area data were obtained by electron microscopy, the additional possibility of systematic error cannot be ignored; for example, fragments of differing size may differ in their degree of adhesion to the EM grid, or very small fragments may not be clearly distinguishable from the background. For these reasons, we are reluctant to place error bars on the area data, so we simply state that a significant fraction of the fragment population would have to remain undetected to alter the $\Delta\chi_{\text{mole}}$ by a factor of two.

A final potential source of error in the estimation of membrane fragment size is the possibility of aggregation of the fragments. In preliminary experiments it was found that the magnetic-field-induced orientation of dilute purple membrane suspensions decreased upon storage at 4°C for periods of more than two weeks. These changes in orientation behavior were believed to result from aggregation of membrane fragments during prolonged storage, and such aggregation was in fact observed by light microscopy. Note that this decrease in magnetic orientation with storage time is consistent only with random, noncoplanar aggregation of the fragments, whereas to produce an increase in the average fragment size and thus in the average diamagnetic anisotropy per particle, the membrane fragments would have to aggregate in a systematic, coplanar fashion. To minimize such artifacts, the experiments reported here were performed within 7 d of isolation of the purple membranes, and microscopic examination of the present samples after completion of the magnetic orientation experiments showed very little clumping. Although it seems likely that any substantial aggregation

would have been detected, the presence of a small population of aggregated fragments cannot be ruled out.

The results presented here show a slightly smaller degree of orientation at 1.7 T than observed by Neugebauer et al. (1977), who reported $\sim 10\%$ orientation of a 2 mg/ml suspension of purple membrane. Similar experiments of the magnetic birefringence of purple membrane suspensions at fields of 1–2 T have recently been carried out by Marrero and Rothschild (Marrero, 1981; Marrero H., and K. Rothschild, manuscript submitted for publication). The difference could arise from variations in either the size or the aggregation state of the membrane fragments, both of which are critical in accurately determining $\Delta\chi_{\text{mole}}$, as shown above. Since the size of purple membrane fragments varies considerably and was not measured in the earlier study, a detailed comparison of these results with those reported here is not possible. As shown above, analysis of experimental results using only the mean fragment size rather than the actual size distribution can lead to significant errors (here $\sim 40\%$) in the final value of $\Delta\chi_{\text{mole}}$. In addition, it should be noted that for measurements carried out only at low fields it is necessary to determine the saturated birefringence separately, which introduces another potential source of error.

Finally, we consider the large variation of b_o with temperature. An S-shaped curve similar to that of Fig. 3 but with an even larger deviation from $1/T$ dependence was observed by Torbet and Maret (1981) for suspensions of the bacteriophages PF1 and fd. To explain this temperature dependence, one can postulate either structural changes or general flexibility changes with temperature. The former possibility has been suggested by some investigators (e.g., Hoffman et al., 1980; Korenstein et al., 1979), who inferred the occurrence of conformational changes in BR with temperature. The latter, flexibility changes with temperature, can occur either at the level of the whole membrane (or phage) or at the molecular level. If the elastic constant for distortion of the membrane shape were a decreasing function of temperature and the magnetic correlation length $\xi_M \geq \langle A_i \rangle^{1/2}$, one would expect larger fluctuations, and therefore a decrease in both b_o and Δn_o , at higher temperatures. With a typical value of $K = 10^{-6}$ erg/cm (Clark et al., 1980), we estimate $\xi_M \equiv (K/\Delta\chi H^2)^{1/2} \approx 0.5 \mu\text{m} \approx \langle A_i \rangle^{1/2}$. However, Δn_o varied by only $\pm 1\%$ around $\Delta n_o = -3.50 \times 10^{-5}$ and showed no systematic change with temperature (Table I), ruling out significant temperature-dependent deviations from flatness.

Flexibility changes at the molecular level would result from an increased degree of vibrational motion of individual groups in the proteins at higher temperatures. For example, with increasing temperature, individual aromatic groups of helices may undergo faster and wider-amplitude librational motions about their equilibrium positions. Evidence for such librational motions of the phenylalanine

rings of BR, increasing with temperature, has been obtained from deuterium nuclear magnetic resonance studies by Rice, D. M., B. A. Lewis, S. Das Gupta, J. Herzfeld, and R. G. Griffin (manuscript in preparation). Such motions will decrease the average diamagnetic and optical anisotropies of the individual groups and thus of the membrane (or phage) as a whole. Either structural or local motional changes could also explain the fact that Torbet and Maret (1981) observed a larger deviation from $1/T$ dependence than seen in the present results. In the bacteriophage the optical anisotropies of the individual groups dominate the observed birefringence, thus effectively squaring the effect of orientation changes or thermal motions of individual groups on the magnetic birefringence; for purple membranes the form birefringence dominates the observed birefringence so that only the diamagnetic anisotropy will be affected by such changes.

In summary, we have measured the magnetic birefringence of dilute purple membrane suspensions as a function of magnetic field strength up to 10.5 Tesla and have independently determined the size distribution of the purple fragments in the suspension. An important feature of the data analysis is the demonstration that an accurate knowledge of the size distribution of the membrane fragments, rather than simply the mean size, is essential to a correct determination of the diamagnetic anisotropy. By including the measured size distribution in a two-parameter fit to the birefringence data, we have calculated a value for the diamagnetic anisotropy per mole of bacteriorhodopsin monomers that suggests a net orientation of the aromatic side chains of BR with their planes perpendicular to the membrane surface. However, given the possibilities of systematic bias in the size determination and of an undetected subpopulation of aggregated membrane fragments, it is difficult to estimate the error bars on this value. It is clear that future studies of similar systems with a wide distribution of particle sizes must carefully address the issue of correctly characterizing the size distribution.

We thank L. Rubin for assistance in scheduling these experiments such that data could be obtained within a few days of sample preparation. We also thank Dr. Barry Stein for assistance with the electron microscopy. In addition, we thank Dr. Kenneth Rothschild for sharing the results of unpublished work from his laboratory, and Dr. E. T. Samulski for useful discussions.

This research was supported in part by the following grants: Office of Naval Research N00014-80-C-0256 (C. Rosenblatt); U. S. Public Health Service (USPHS) Postdoctoral Fellowship GM 09062 (B. A. Lewis); USPHS GM 23316 (J. Herzfeld); and USPHS GM 23289 (R. G. Griffin). The Francis Bitter National Magnet Laboratory is supported by a grant from the National Science Foundation, Division of Materials Research (DM-8211416).

Received for publication 5 April 1984 and in final form 27 September 1984.

REFERENCES

- Abramowitz, M., and I. A. Stegun. 1972. Handbook of Mathematical Functions. National Bureau of Standards, Washington, DC.
- Argade, P. V., K. J. Rothschild, A. H. Kawamoto, J. Herzfeld, and W. C. Herlihy. 1981. Resonance Raman spectroscopy of specifically ^{15}N lysine-labeled bacteriorhodopsin. *Proc. Natl. Acad. Sci. USA.* 78:1643-1646.
- Becher, B., F. Tokunaga, and T. G. Ebrey. 1978. Ultraviolet and visible absorption spectra of the purple membrane protein and the photocycle intermediates. *Biochemistry.* 17:2293-2300.
- Blaurock, A. E. 1975. Bacteriorhodopsin: a trans-membrane pump containing α -helix. *J. Mol. Biol.* 93:139-158.
- Blaurock, A. E., and W. Stoerkenius. 1971. Structure of purple membrane. *Nat. New Biol.* 233:152-155.
- Bogomolni, R. A., L. Stubbs, and J. K. Lanyi. 1978. Illumination-dependent changes in the intrinsic fluorescence of bacteriorhodopsin. *Biochemistry.* 17:1037-1041.
- Born, M., and E. Wolf. 1980. Principles of Optics. Pergamon Press, Oxford.
- Boroske, E., and W. Helfrich. 1978. Magnetic anisotropy of egg lecithin membranes. *Biophys. J.* 24:863-868.
- Brith-Lindner, M., and K. Rosenheck. 1977. The circular dichroism of bacteriorhodopsin: asymmetry and light-scattering distortions. *FEBS (Fed. Eur. Biochem. Soc.) Lett.* 76:41-44.
- Clark, N. A., K. J. Rothschild, D. A. Luippold, and B. A. Simon. 1980. Surface-induced lamellar orientation of multilayer membrane arrays. *Biophys. J.* 31:65-96.
- Cross, T. A., and S. J. Opella. 1983. Protein structure by solid-state NMR. *J. Am. Chem. Soc.* 105:306-308.
- DeGennes, P. G. 1975. Physics of Liquid Crystals. Clarendon Press, Oxford.
- Draheim, J. E., N. J. Gibson, S. C. Hartsel, and J. Y. Cassim. 1984. A deformation wave model for the photoinduced transmembrane vectorial proton transport in the purple membrane. *Biophys. J.* 45(2, Pt. 2):211a. (Abstr.)
- Ekiel, I., D. Marsh, B. W. Smallbone, M. Kates, and I. C. P. Smith. 1981. The state of the lipids in the purple membrane of *Halobacterium cuturubrum* as seen by ^{31}P NMR. *Biochem. Biophys. Res. Commun.* 100:105-110.
- Fukumoto, J. M., and M. A. El-Sayed. 1983. Absorption polarization properties of light-adapted bacteriorhodopsin in the 266-620 nm region. *Photochem. Photobiol.* 38:79-82.
- Henderson, R. 1975. The structure of the purple membrane from *Halobacterium halobium*: analysis of the x-ray diffraction pattern. *J. Mol. Biol.* 93:123-138.
- Henderson, R. 1977. The purple membrane from *Halobacterium halobium*. *Annu. Rev. Biophys. Bioeng.* 6:87-109.
- Henderson, R., and P. N. T. Unwin. 1975. Three-dimensional model of purple membrane obtained by electron microscopy. *Nature (Lond.)* 257:28-32.
- Hess, B., and D. Kuschmitz. 1979. Kinetic interaction between aromatic residues and the retinal chromophore of bacteriorhodopsin during the photocycle. *FEBS (Fed. Eur. Biochem. Soc.) Lett.* 100:334-339.
- Heyn, M. P., P.-J. Bauer, and N. A. Dencher. 1975. A natural CD label to probe the structure of the purple membrane from *Halobacterium halobium* by means of exciton coupling effects. *Biochem. Biophys. Res. Commun.* 67:897-903.
- Hoffman, W., M. Graca-Miguel, P. Barnard, and D. Chapman. 1980. *FEBS (Fed. Eur. Biochem. Soc.) Lett.* 95:31-34.
- Jap, B. K., M. F. Maestre, S. B. Hayward, and R. M. Glaeser. 1983. Peptide-chain secondary structure of bacteriorhodopsin. *Biophys. J.* 43:81-90.
- Khorana, H. G., G. E. Gerber, W. C. Herlihy, C. P. Gray, R. J. Andereg, K. Nihei, and K. Biemann. 1979. Amino acid sequence of bacteriorhodopsin. *Proc. Natl. Acad. Sci. USA.* 76:5046-5050.

- Knox, R. S., and M. A. Davidovich. 1978. Theory of fluorescence polarization in magnetically oriented photosynthetic systems. *Biophys J.* 24:689-712.
- Korenstein, R., B. Hess, and M. Markus. 1979. *FEBS (Fed. Eur. Biochem. Soc.) Lett.* 102:155-161.
- Marrero, H. 1981. Determination of the volumetric diamagnetic anisotropy of bacteriorhodopsin. Masters thesis. Boston University, Boston, MA.
- Murthy, N. S., J. R. Knox, and E. T. Samulski. 1976. Order parameter measurements in polypeptide liquid crystals. *J. Chem. Phys.* 65:4835-4839.
- Neugebauer, D.-Ch., A. E. Blaurock, and D. L. Worcester. 1977. Magnetic orientation of purple membranes demonstrated by optical measurements and neutron scattering. *FEBS (Fed. Eur. Biochem. Soc.) Lett.* 78:31-35.
- Oesterhelt, D., and W. Stoeckenius. 1971. Rhodopsin-like protein from the purple membrane of *Halobacterium halobium*. *Nat. New Biol.* 233:149-154.
- Oesterhelt, D., and W. Stoeckenius. 1974. Isolation of the cell membrane of *Halobacterium halobium* and its fractionation into red and purple membrane. *Methods Enzymol.* 31:667-678.
- Ovchinnikov, Yu. A., N. G. Abdulaev, M. Yu. Feigina, A. V. Kiselev, and N. A. Lobanov. 1979. The structural basis of the functioning of bacteriorhodopsin: an overview. *FEBS (Fed. Eur. Biochem. Soc.) Lett.* 100:219-224.
- Pauling, L. 1979. Diamagnetic anisotropy of the peptide group. *Proc. Natl. Acad. Sci. USA.* 76:2293-2294.
- Rosenblatt, C. 1984. Temperature dependence of the anisotropic potential at a nematic liquid crystal — wall interface. *J. Physique.* 45:1087-1092.
- Rosenblatt, C., and J. T. Ho. 1982. Birefringence investigation of the smectic A — Hexatic B transition. *Phys. Rev. A.* 26:2293-2296.
- Sakurai, I., Y. Kawamura, A. Ikegami, and S. Iwayanagi. 1980. Magneto-orientation of lecithin crystals. *Proc. Natl. Acad. Sci. USA.* 77:7232-7236.
- Scholz, F., E. Boroske, and W. Helfrich. 1984. Magnetic anisotropy of lecithin membranes. *Biophys. J.* 45:589-592.
- Stoeckenius, W. 1980. Purple membrane of halobacteria: a new light-energy converter. *Acc. Chem. Res.* 10:337-344.
- Stoeckenius, W., and R. A. Bogomolni. 1982. Bacteriorhodopsin and related pigments of halobacteria. *Annu. Rev. Biochem.* 52:587-616.
- Torbet, J., and G. Maret. 1981. High-field magnetic birefringence study of the structure of rodlike phages Pf1 and fd in solution. *Biopolymers.* 20:2657-2669.
- Wallace, B. A. 1982. Comparison of bacteriorhodopsin and rhodopsin molecular structure. *Methods Enzymol.* 88:447-462.
- Worcester, D. L. 1978. Structural origins of diamagnetic anisotropy in proteins. *Proc. Natl. Acad. Sci. USA.* 75:5475-5477.